Acta orthop. scand. 48, 250–262, 1977

THE EFFECT OF IMPACT LOADING ON RABBIT KNEE JOINTS

M. T. SERINK, A. NACHEMSON & G. HANSSON

Department of Orthopaedic Surgery I and the Department of Pathology II, Sahlgren Hospital, Göteborg, Sweden.

Eighteen mature male Whiteland rabbits received repetitive impulse loads slightly larger than body weight (4 kp) through one knee joint for periods from 1 to 6 weeks. Mechanical compression of subchondral bone cores from impacted tibiae showed progressive increased deformation under a constant force. Cartilage degeneration occurred concurrently with alterations in the mechanical properties of the subchondral bone. The cartilage degeneration may be explained by: (i) the deleterious effect of repetitive mechanical compression, (ii) the decreased mechanical support of the underlying subchondral bone.

Key words: subchondral bone; microfractures; fatigue; impact loading; reflected light microscopy

Accepted 21.i.77

Despite a multitude of factors known to be responsible for the induction of both clinical and experimental degenerative joint disease, the etiology of primary osteoarthritis remains unsolved (Gardner 1960).

The attenuation across joints of forces resulting from impact loads has been shown to be a function of subchondral bone and soft tissue rather than cartilage or synovial fluid (Radin et al. 1970). A current hypothesis concerning the etiology of degenerative joint disease proposes that microfractures occur in subchondral bone as a result of repetitive impact loads. These lead to subchondral bone stiffening secondary to callus formation (Radin et al. 1973). This stiffening of the subchondral bone presumably reduces its shock absorbing qualities, which then predisposes the overlying cartilage to degeneration.

The purpose of this study is 1) to produce experimental degenerative joint disease secondary to impact loading and 2) to examine the changes occurring in the affected tissues, particularly the subchondral bone.

MATERIALS AND METHODS

Loading machine

An experimental machine was designed, which loaded the right knee joint of six rabbits simultaneously (Figure 1). Both legs were held in extension at the knee joint with plastic splints. The right leg of each animal was subjected to a 4 kp impulse load 56 times per minute for 1 hour daily. The frequency and amplitude of the impact load were selected so as to simulate the work of Radin et al. (1973). The left knee of each animal served as a control and was not loaded.

A schematic drawing of how the cyclic impulse load was delivered is shown in Figure 2. The springs used to produce the 4 kp load were specially constructed to produce this force with 5 mm of deformation. All springs were tested

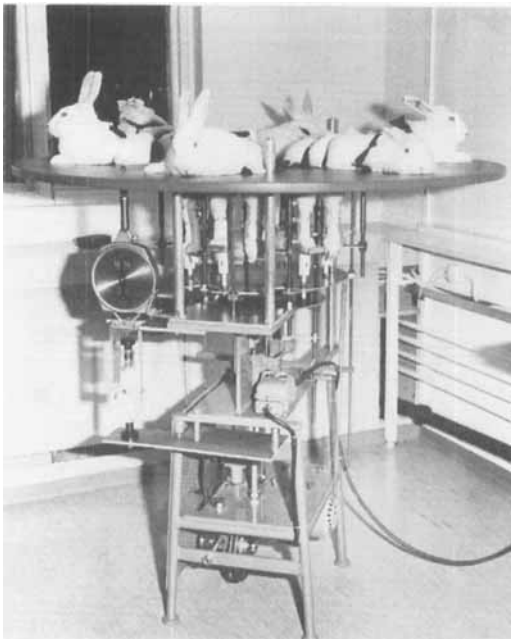

Figure 1. Six rabbits are shown in the impulse loading machine. The right leg of each rabbit received a 4 kp load 56 times per minute. The left leg was not loaded and served as a control.

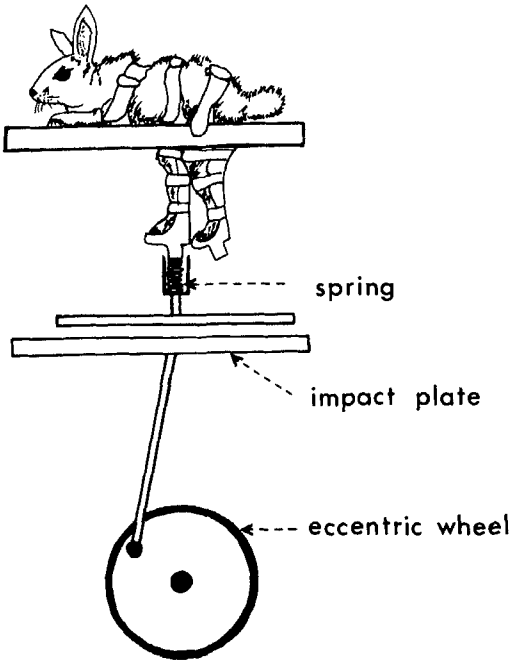

Figure 2. A schematic drawing showing how the impulse load was produced and transmitted to the right leg of each rabbit. Special springs were constructed to produce 4 kp of force with 5 mm of deformation.

for error prior to and at the completion of the experiment—this was found to be ± 1 per cent. The height of the cylinders in which the springs were housed was made adjustable to accommodate anatomical variations in the rabbits' legs.

The relationship of force input to time is depicted by a dome-shaped curve (Figure 3). The impulse load of each cycle started at 0.07 sec, rose to 4 kp at 0.28 sec and then decreased to 0 kp of force at 0.49 sec. The total duration of the impulse was 0.42 sec.

The rapid rise and fall of this force-time relationship was chosen to simulate clinical stresses occurring in the human knee joint while walking (Morrison 1970).

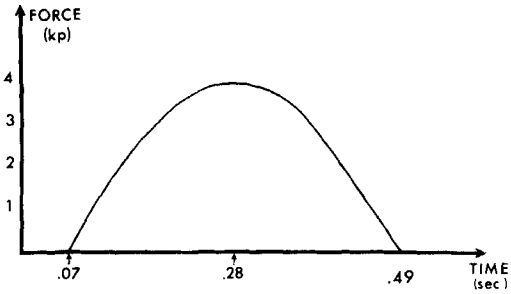

Figure 3. The dome shaped curve represents the force input into the right leg with each impulse load. This impulse load occurred 56 times per minute for 1 hour daily. The rapid rise and fall of the force input was selected to simulate joint loads which occur clinically.

Animal selection

Eighteen male Whiteland rabbits weighing from 2.5–3 kg were divided into six groups containing three animals each. Each group was then tested for time intervals from 1 to 6 weeks. The knee joints of all animals were X-rayed prior to testing to ensure skeletal maturity. All animals were allowed free movement in their cages except for the 1 hour of daily impact loading.

Experimental procedure

A general outline of the experimental procedure followed is shown in Figure 4.

Tibial cores

At the completion of each week of loading, three animals were sacrificed and both knee

joints were disarticulated. The proximal ends of the tibiae were then placed in plastic molds to fix the sites of the cores. With a 5 mm trephine drill, under cooling irrigation, a core was removed from each medial tibial condyle. The core was then machined in a turning lathe with an optical microscope attached to ensure complete removal of all cartilage. A special chuck with a face-plate backing ensured that both surfaces of the specimen were parallel. The length of the core was 3 ± 0.05 mm.

Mechanical testing

An Alwetron testing machine compressed the tibial cores to a maximum of 1 kp of force (error ± 1 per cent). The rate of compression was 0.05 mm/min. The deformation of each core was simultaneously read in a recorder and a load deformation curve was thus obtained (Figure 5).

Each sample was measured with a micrometer (± 0.01 mm) before and after testing. The permanent deformation produced by the mechanical compression is recorded in Table 1.

All samples were stored in normal saline at room temperature prior to testing. The time interval from sacrifice of the animal to testing was approximately 6 hours.

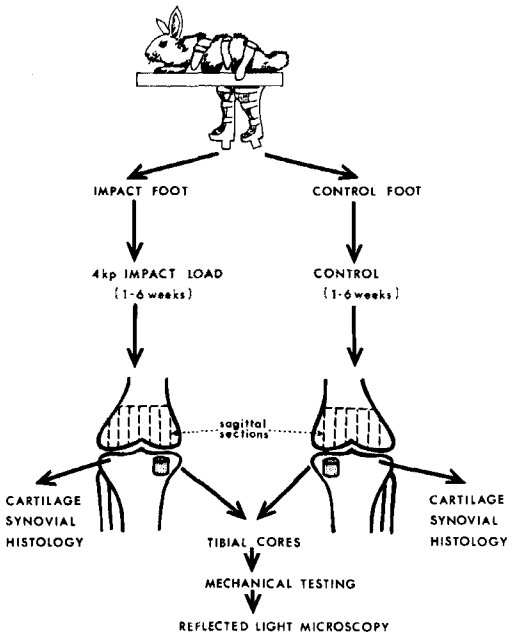

Figure 4. A schematic outline of the experimental procedure followed.

Table 1. The mechanical deformation of the control and loaded tibial cores. The permanent deformation produced by mechanical compression is recorded in column 8 and is measured in microns. The higher incidence of permanent deformation occurring on the loaded as opposed to the control side should be noted.

Rabbit	1 week		2 weeks		3 weeks		4 weeks		5 weeks		6 weeks		Perm. def.	
	contr.	load	contr.	load	contr.	load	contr.	load	contr.	load	contr.	load	contr.(μ)	load
1	22.4	12.6											0	0
2	25.3	28.0											0	0
3	20.0	28.0											0	0
4			13.0	29.5									0	40
5			26.0	18.0									0	0
6			22.0	24.0									0	10
7					19.5	25.0							0	10
8					21.5	22.0							0	10
9					20.5	26.0							10	10
10							16.0	22.5					10	10
11							17.0	22.5					0	0
12							27.5	40.0					0	0
13									22.5	40.0			0	10
14									15.0	22.5			0	0
15									28.0	41.0			0	0
16											17.5	22.5	0	20
17											18.0	35.0	0	20
18											18.0	35.0	0	30

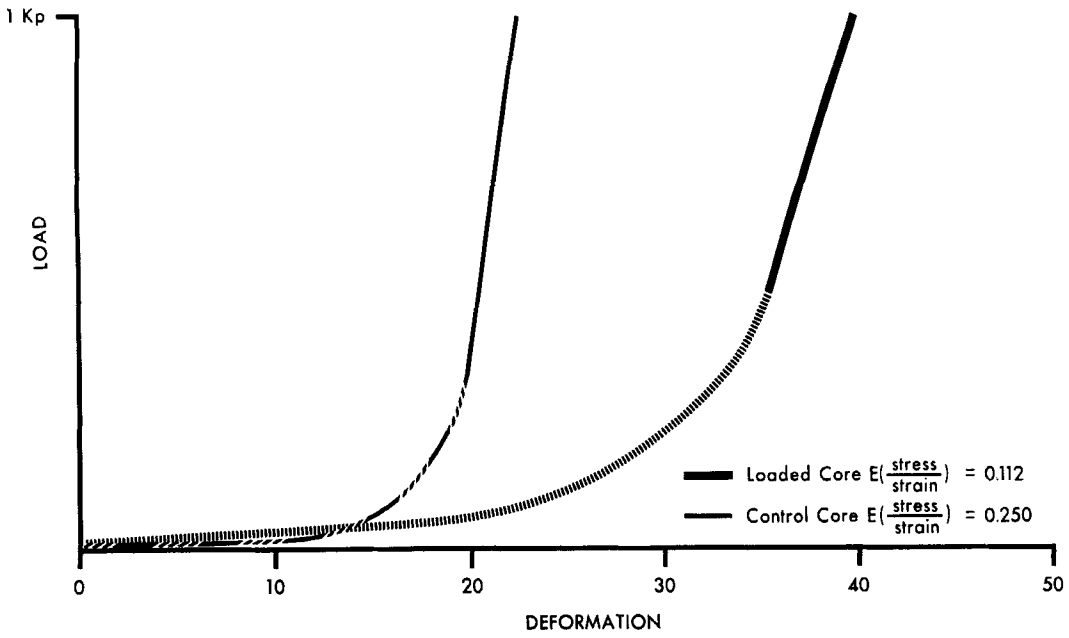

Figure 5. This is a graphic representation of the load/deformation curve obtained from the Alwetron testing machine. These curves refer to the control and impact loaded tibial cores from a rabbit subjected to 5 weeks of impact loading (see Table 1, rabbit 13). The units of deformation correspond to the squares of the actual graph paper output from the Alwetron. These can be converted to absolute values (mm) by dividing by 324. The non-linear portion (broken lines) of each curve represents the "seating in" of the core during initial mechanical compression. The linear portion (solid line) of each curve depicts elastic deformation of the tibial cores. By calculating the slopes of these solid lines we can then compare the relative modulus of elasticity or stiffness between the impact loaded and control cores.

$$\textit{Control core}\quad E\left(\frac{\text{stress}}{\text{strain}}\right) = \text{slope} = \frac{1\text{ kilopond}}{22.5 - 18.5} = 0.250$$

$$\textit{Impact loaded core}\quad E\left(\frac{\text{stress}}{\text{strain}}\right) = \text{slope} = \frac{1\text{ kilopond}}{40 - 31.1} = 0.112$$

The slopes of each curve are in load/deformation units. Since each core was standardized for length and cross-sectional area, these values are directly proportional to absolute stress/strain units (i.e. modulus of elasticity).

Femoral condyles

The right and left distal femurs were cut sagittally to a depth of 15 mm and a thickness of 2 mm under cooling irrigation (Figure 4).

Histology

1) *Synovium.* Synovial biopsies of both knees were fixed in 4 per cent neutral formalin and then stained with hematoxylin and eosin and van Gieson.

2) *Cartilage.* The lateral tibial condyles were fixed in 4 per cent neutral formalin, decalcified in Parengy solution, and stained with Tolidine blue at pH 0.5 and 4.0, hematoxylin and eosin and van Gieson.

3) *Tibial cores and femoral slices.* These samples were first defatted in solutions of ethyl alcohol and ether. The liquid component of the bone was removed by vacuum drying. The specimens were then embedded in epoxy resin (Araldit D*) under vacuum (Luft 1961). The specimens obtained were ground with wet silica carbide paper, polished, and then subjected to reflected light microscopy (Pugh et al. 1972).

Limitations of present study

1) *Force input.* Although the cylinders were adjustable to accommodate anatomical variations

* (Araldit D CY 230 Ciba).

in each rabbit leg, the error in force input could not be controlled to better than ± 500 g.

2) *Tibial cores.* The use of plastic molds standardized the size and angle for selection of each core from the medial tibial condyle. Anatomical variations in the size of tibiae introduced an unavoidable error.

3) *Permanent deformation.* The amount of permanent deformation produced by compressing the bone with 1 kp of force is recorded in Table 1 (column 8). This deformation is produced by breaking the bone. Artifactual cracks thus result from this testing procedure. However, since our criteria of a true microfracture included the demonstration of callus, breaks resulting from artifact would be excluded.

RESULTS

1) *Gross examination of tibial cores*

The impacted tibial cores became more friable and developed a texture analogous to granular sugar as the experiment progressed. These changes were not noted on the control side.

2) *Mechanical compression of tibial cores*

Figure 5 is a graphic representation of the load deformation curve obtained from the Alwetron testing machine. The deformation curves refer to the control and impact loaded tibial cores from a rabbit tibia subjected to 5 weeks of impact loading. These curves allow the comparison of relative stiffness (modulus of elasticity) between an impact loaded and a control core. The modulus of elasticity of the control core is 0.250 while that of the impacted core is 0.112 (Figure 5).

No significant difference was found between the impacted and control tibial cores in the first 2 weeks of loading (Table 1). This is attributable to the minimal difference in the average deformation values between the impacted and control groups (Sign and Walsh Test, Siegel 1956). In the 3, 4, and 5 week groups

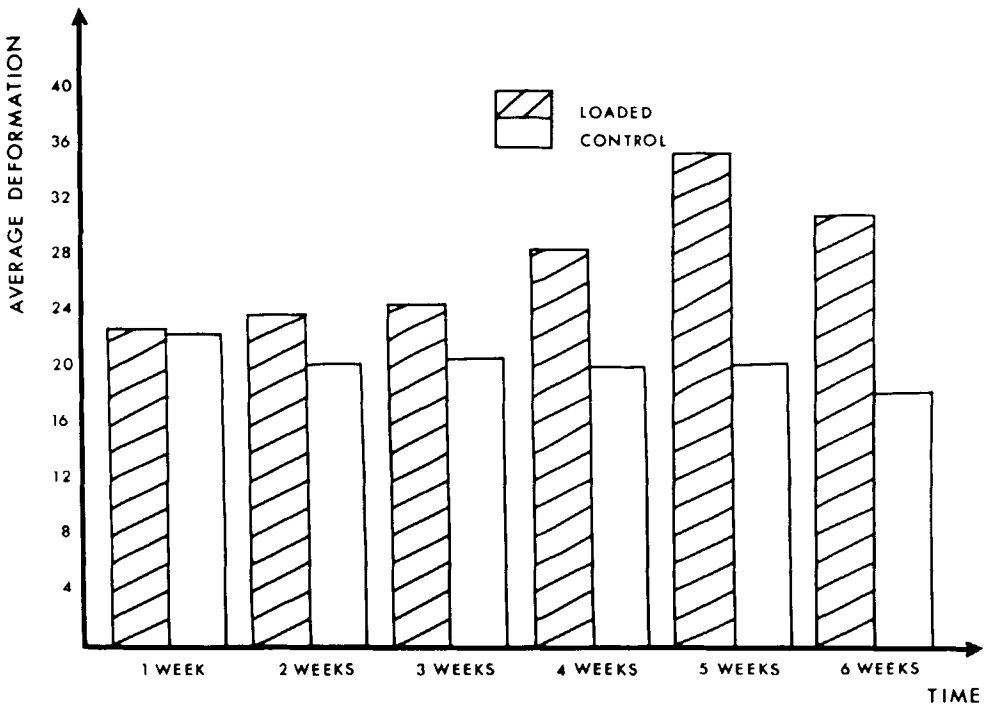

Figure 6. Bar graph showing the average mechanical deformation of the control and loaded tibial cores with time.

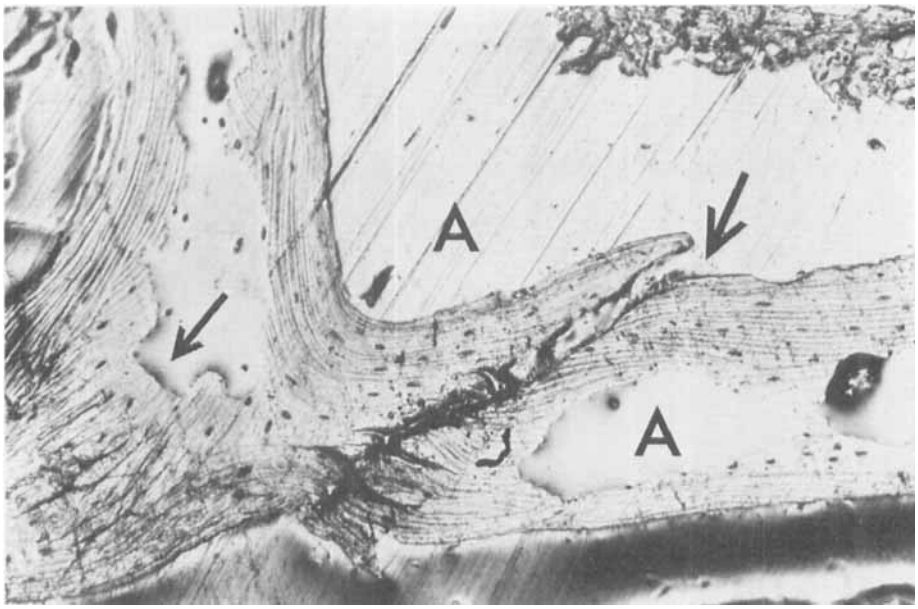

Figure 7. Photomicrograph of a cancellous bone trabecula subjected to reflected light microscopy (× 55). This specimen is taken from a 3-week impacted tibial core. The arrows show artifactual cracks produced either by the machining or the mechanical testing of the specimen. Note the absence of callus. "A" denotes the epoxy resin in which the specimen is embedded. The dark diagonal lines seen crossing the specimen are artifacts produced during polishing.

there were statistically significant differences between the impacted cores on a 1.6 per cent level.

The mechanical deformations of the control and tested tibial cores at weekly intervals are also shown in Table 1. In all rabbits (except for rabbits one and five) the deformation observed in the loaded cores exceeded that in the control group. As the cancellous bone became more deformable, the mechanical deformation increased (Figure 5).

The average deformation of the tibial cores progressively increased over the 6-week period (Figure 6). The average deformation for the 1, 3, and 6 week impacted group was 22.9, 24.3, and 30.8 units.

3) *Permanent deformation*

The amount of permanent deformation in the tibial cores following the 1 kp of mechanical force is recorded in Table 1 (column 8). Permanent deformation occurred in 12 of the 36 cores tested. Of these, ten occurred in the loaded tibial cores, the remaining two in the control cores.

4) *Reflected light microscopy of tibial cores*

Reflected light microscopy demonstrated numerous artifactual cracks to be present in all tibial cores. These occurred either in preparation of cores or during mechanical compression.

A cancellous core from a 3-week impacted tibia is shown in Figure 7. The crack in the trabecula is indicative of an artifact because it lacks callus formation. A photograph of an impacted tibial core from a 5-week animal is shown in Figure 8. This crack is suggestive of a healing microfracture in that it displays periosteal swelling. The lack of cellular activity is related to the preparation of the specimen.

In general the number of artifac-

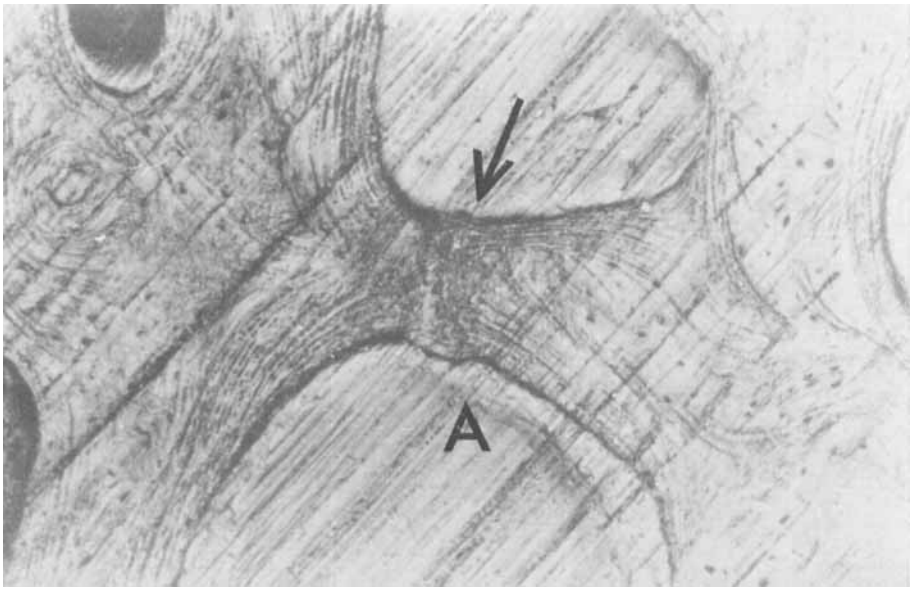

Figure 8. Photomicrograph of cancellous bone taken from a 5-week impacted tibial core (reflected light microscopy × 42). The fatigue fracture depicted by the arrow shows periosteal reaction indicative of callus formation. Note the lack of displacement at the fracture site.

tual cracks occurring in the control tibial cores remained relatively constant throughout the experiment. The impacted cores, however, tended to show an increase in artifactual cracks as the experiment progressed. Trabecular fractures associated with periosteal reaction as depicted in Figure 8 were absent from the control cores and did not appear in any of the impacted cores until 2 weeks of loading. It must be stressed, however, that their occurrence was rare and did not seem to increase with the duration of loading. Of all the specimens examined, only two examples of the microfracture shown were found.

5) *Reflected light microscopy of femoral slices*

The frequency of artifactual cracks on the control side remained constant while the loaded side showed a progressive increase of artifacts with time. However, no evidence of fractures associated with callus formation were seen in any of these specimens.

6) *Histology of synovial membrane*

A. Gross. After the first week of impulse loading the impacted knees developed synovial effusions, which were progressive with time and associated with gradual atrophy of the synovial membrane and steady thickening of the joint capsule.

B. Microscopic examination. The normal synovial membrane has a loose connective tissue stroma (Figure 9) and the first changes in the experimental synovial membrane occurred in this stroma. The loose stroma was gradually replaced by cellular connective tissue with collagen fibers (Figure 10). A progressive increase in capillary vessels in the synovial villi occurred and in some areas there was hyperplasia of the synovial epithelium. In all impact loaded rabbits, by the 6-week period, foreign body giant cells were seen in the synovial stroma and pericapsular tissue (Figure 11). Van Kossa stain revealed that some of these giant cells contained calcium.

The synovial membrane of the control

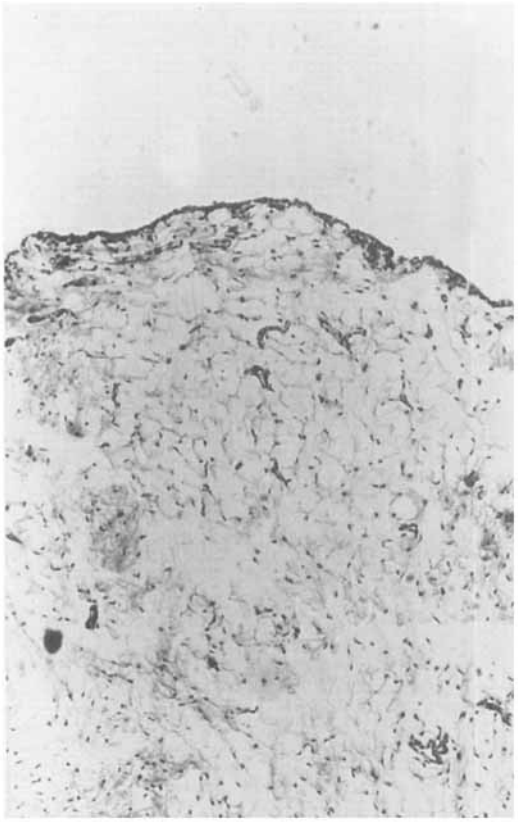

Figure 9. Photomicrograph of normal synovial membrane taken from a 3-week control knee joint (hematoxylin and eosin × 38).

side remained normal both grossly and microscopically.

7) *Histology of articular cartilage*

A. Gross. The impacted articular cartilage of the tibia and femur showed a gradual loss of the glistening, shiny, blue-white appearance of normal cartilage. Changes were noted by the end of the first week of testing and there was a gradual progression to a non-glistening, yellow, fibrillated surface accompanied in the later stages with lipping of the joint margins.

No changes were noted in the control knees.

B. Microscopic examination. Histological examination with hematoxylin and eosin and Tolidine blue at pH 0.5 and 4.0 failed to reveal any appreciable abnormality in the first 2 weeks of loading.

At the completion of the third week, examination of the periarticular cartilage showed derangement of the columnar pattern of cartilage cells. Fibrillation of the articular cartilage, characterized by disruption of the matrix with cleft formation and deletion of ground substance, as revealed with Tolidine blue stain, was also noted (Figures 12 and 13).

Increased vascularity of the subchondral bone was accompanied by invasion

Figure 10. Photomicrograph of synovial membrane taken from a 3-week impacted knee joint (hematoxylin and eosin × 32). Note increased collagen.

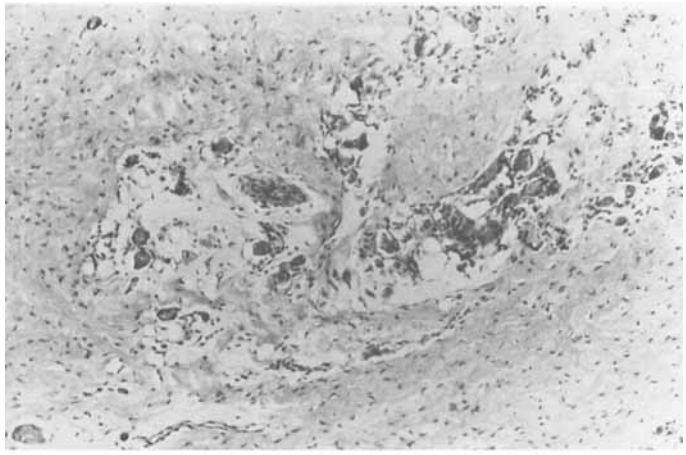

Figure 11. Photomicrograph of pericapsular area in a 6-week impacted knee joint showing foreign body giant cells (hematoxylin and eosin × 32).

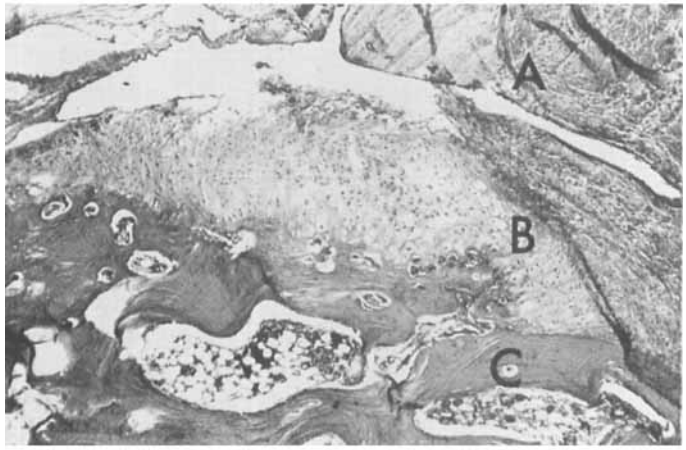

Figure 12. Photomicrograph of degenerating periarticular cartilage taken from a 3-week loaded tibia. "A" denotes capsule, "B" periarticular cartilage, "C" subchondral bone (hematoxylin and eosin × 15).

Figure 13. Higher magnification of Figure 12 showing marrow and blood vessels from the subchondral bone invading the zone of calcified cartilage (hematoxylin and eosin × 32).

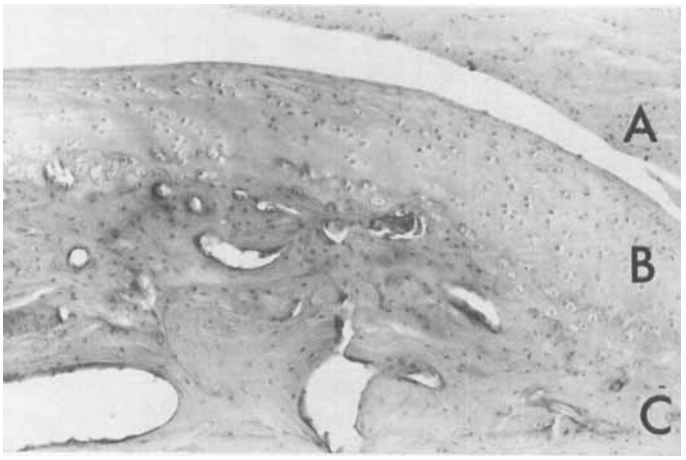

Figure 14. Photomicrograph of normal periarticular tibial cartilage from a 3-week control animal. "A" denotes capsule, "B" cartilage and "C" subchondral bone (hematoxylin and eosin × 15).

of blood vessels into the cartilage (Figure 13). Periarticular cartilage from the control tibia is shown in Figure 14.

DISCUSSION

Previous studies

Radin and co-workers using a similar experimental model found that repetitive impact loading of rabbit knee joints resulted in subchondral bone stiffening (Radin et al. 1973). They proposed that this stiffening is due to healing microfractures occurring consequent to repetitive impact loads. It has also been suggested that cartilage degeneration is preceded by and attributable to stiffening of the subchondral bone.

Their work, however, appears to suffer from two limitations. Firstly, the rabbit cartilage on which they based their conclusions was distal femoral while the subchondral bone used was proximal tibial. Statements relating subchondral bone stiffness to cartilage degeneration are therefore not necessarily valid (Radin et al. 1973). Secondly, they have reported subchondral bone stiffening, secondary to callus formation, as early as the sixth day during impact loading. Mechanical studies of fracture healing in rabbits have shown that the original strength of the fracture is not regained until the seventeenth day post-fracture (Brighton & Krebs 1972).

Lereim et al. (1974) studying patients with rheumatoid and osteoarthritis of the knee found that the hardness of the subchondral bone was significantly less in these subjects than in normal bone.

Subchondral bone changes

The findings in this study indicate that repetitive impact loading through rabbit knee joints results in a progressive increase in the deformability of the subchondral bone under a constant force. This is supported by the steady rise in the average deformation values of the impacted subchondral bone cores with time (Figure 6). The higher value of the modulus of elasticity in the control tibial core as opposed to the impacted core suggests that subchondral bone softening occurs with impact loading (Figure 5). The increased incidence of permanent deformation in the impacted cores (10) as opposed to the control (2) also suggests that the impacted bone was not as strong as the control.

Etiology of subchondral bone changes

No definite explanation for the changes noted in the subchondral bone is proposed from this work. Osteoporosis (decreased

inorganic bone matrix) secondary to hyperemia of the subchondral bone could account for the increased fragility of the impacted tibial cores (Figure 13). This is supported by the work of Harrison et al. (1953). They have shown, in osteoarthritic femoral heads, that vascular proliferation and marrow invasion result in osteoporosis. Seireg & Kemple (1969), however, found no change in the mineral or collagen content of rat tibiae subjected to prolonged cyclic loading.

The reaction of the synovial membrane in this experimental model is thought to be non-specific, although local or metabolic factors may have been induced. These could account for the changes seen.

The increasing deformation of the cancellous bone may have a more complex etiology. Since each loaded knee received 16,800 impacts per week, fatigue failure of individual trabeculae may be responsible. Fatigue fractures have been produced experimentally in cadaveric human femoral necks with cyclic loads approximating four times body weight (Griffiths et al. 1971). While not conclusive, the abnormal trabecular seen in Figure 8 is suggestive of fatigue fractures. The lack of displacement coupled with the periosteal reaction resembles a fatigue fracture occurring in clinical practice. Absence of cellular activity may be explained by the preparation of the specimen, since the reflected light microscopy technique has the advantage of retaining the structural integrity of cancellous bone, but distorting the cellular detail. As a result, the cellular component of callus may be absent (Pugh et al. 1972).

Isolated trabecular fatigue fractures of human femoral necks occurring in subchondral bone in association with osteoarthritis, rheumatoid arthritis, and subcapital fractures have been reported (Todd et al. 1972).

It is unlikely that fatigue fractures can fully explain the etiology of the subchondral bone changes. It should be stressed that their occurrence was rare and did not increase in frequency as the mechanical deformation increased.

Etiology of articular cartilage changes

The mechanism of cartilage degeneration with impulse loading is likewise unclear. Direct pressure is known to be incompatible with cartilage survival, presumably because of interference with nutrition (Salter & Field 1969). Repetitive loading may also interfere with cartilage survival by expressing a small amount of water from the matrix with each cycle. This results in a gradual diminution of the viscous component of dampening thus exposing the matrix to mechanical deformation and degeneration (Freeman 1973). Fatigue of cartilage produced experimentally is not associated with mucopolysaccharide depletion (Weightman et al. 1973).

Harrison et al. (1953) studying osteoarthritis in human femoral heads showed that there is early invasion of cartilage by marrow and subchondral blood vessels. They emphasize that this invasion first occurs in non-weightbearing areas. The periarticular non-weightbearing area from a 3-week impacted tibia supports this view (Figures 12 and 13). It must be emphasized that the hyperemia seen in the subchondral bone is non-specific and may be a local reaction to trauma.

Relationship of subchondral bone changes to cartilage degeneration

Increased deformability of the subchondral bone would result in decreased structural support of the overlying cartilage. Articular cartilage devoid of support would be subject to collapse under loading. This could produce high stress concentrations both internally and tangentially thus resulting in fatigue of cartilage.

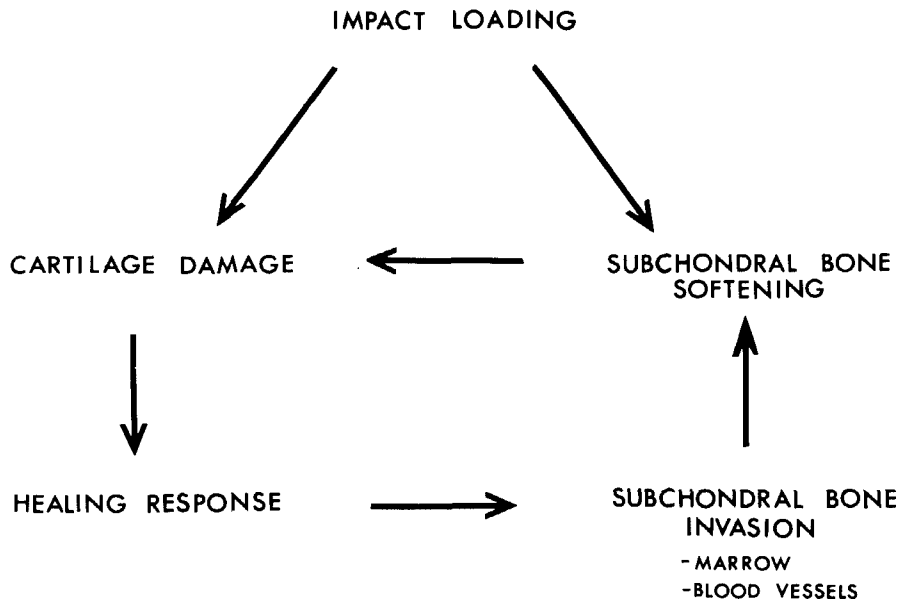

Figure 15. Diagram summarizing proposed mechanisms of experimental degenerative joint disease secondary to cyclic impact loading.

The time relationship between cartilage and subchondral bone changes in experimental degenerative joint diseases is open to three theoretical pathways. Following induction by impulse loading, cartilage degeneration may precede, follow or occur simultaneously with subchondral bone changes.

This work supports the concept that subchondral bone changes and cartilage degeneration occur concurrently in joints subjected to mechanical trauma by impact loading. Cartilage and subchondral changes were not seen until the third week of testing.

A summary of the proposed mechanism of experimental degenerative joint disease secondary to impact loading is shown in Figure 15.

SUMMARY

1) Eighteen male mature Whiteland rabbits received repetitive impulse loads slightly larger than body weight through one knee joint for periods of 1 to 6 weeks.

2) The subchondral bone cores from impacted tibiae showed progressive increased deformability under a constant force.

3) Reflected light microscopy showed evidence of fatigue fractures occurring in trabecula from the impacted tibiae.

4) The increased deformability of the impacted subchondral bone may be related to osteoporosis secondary to hyperemia.

5) Cartilage studies from impacted tibiae suggest that degeneration occurs concurrently with alterations in the mechanical properties of the subchondral bone.

6) Cartilage degeneration occurred first and with greater severity in non-weightbearing areas of the articular cartilage.

7) This mechanical model supports the view that cartilage degeneration may be affected by:

(i) the direct effect of repetitive mechanical compression, i.e. fatigue.

(ii) the decrease in mechanical support of the subchondral bone.

ACKNOWLEDGMENTS

This work was sponsored by the Medical Research Council of Canada and Ulla and Gustaf av Ugglas fund, Karolinska Institute, Stockholm, Sweden. Special tribute is also paid to Jurek Lankiewicz and Jaromir Agneskans at Chalmers University of Technology, Göteborg, Sweden, for their assistance. Drawings and graphs were contributed by Sten Holm.

REFERENCES

Brighton, C. T. & Krebs, A. G. (1972) Oxygen tension of healing fractures in the rabbit. *J. Bone Jt Surg.* **54**-A, 323–332.

Freeman, M. A. R. (1973) *Adult articular cartilage.* Ed. Freeman, M. A. R. pp. 33–245. Sir Isaac Pitman and Sons Ltd., London.

Gardner, D. L. (1960) The experimental production of arthritis. *Ann. Rheum. Dis.* **19**, 297–305.

Griffiths, W. E., Swanson, S. A. V. & Freeman, M. A. R. (1971) Experimental fatigue fracture of the human cadaveric femoral neck. *J. Bone Jt Surg.* **53**-B, 136–143.

Harrison, M. H. M., Schajowicz, F. & Trueta, J. (1953) Osteoarthritis of the hip: A study of the nature and evolution of the disease. *J. Bone Jt Surg.* **35**-B, 598–626.

Lereim, P., Goldie, I. & Dahlberg, E. (1974) Hardness of the subchondral bone of the tibial condyles in the normal state and in osteoarthritis and rheumatoid arthritis. *Acta orthop. scand.* **45**, 614–627.

Luft, J. H. (1961) Improvements in epoxy resin embedding methods. *J. biophys. biochem. Cytol.* **9**, 409–414.

Morrison, J. B. (1970) The mechanics of the knee joint in relation to normal walking. *J. Biomech.* **3**, 51–61.

Pugh, J., Rose, R. & Radin, E. (1972) Techniques for the study of the structure of bone. *Microstructures* **3**, 23–27.

Radin, E., Parker, H. G., Pugh, J., Steinberg, R. S., Paul, I. G. & Rose, R. (1973) Response of joints to impact loading—III. *J. Biomech.* **6**, 51–57.

Radin, E., Paul, I. G. & Lowy, M. (1970) A comparison of the dynamic force transmitting properties of subchondral bone and articular cartilage. *J. Bone Jt Surg.* **52**-A, 444–456.

Salter, R. D. & Field, P. (1969) The effects of continuous compression on living articular cartilage. *J. Bone Jt Surg.* **42**-A, 31–49.

Seireg, A. & Kempke, W. (1969) Behavior of in vivo bone under cyclic loading. *J. Biomech.* **2**, 455–461.

Siegel, S. (1956) *Non parametric statistics for the behavioral sciences.* McGraw-Hill Book Co. Inc., Kogakusha Co. Ltd., Tokyo.

Simon, P. S., Radin, E., Paul, I. G. & Rose, R. (1972) Response of joints to impact loading. II. In vivo behavior of subchondral bone. *J. Biomech.* **5**, 267–272.

Todd, R. C., Freeman, M. A. R. & Pirie, C. J. (1972) Isolated trabecular fatigue fractures in the femoral head. *J. Bone Jt Surg.* **54**-B, 723–728.

Weightman, B. O., Freeman, M. A. R. & Swanson, S. A. V. (1973) Fatigue of articular cartilage. *Nature (Lond.)* **244**, 303–304.

Correspondence to: Dr. M. T. Serink, 325-5000 Kingsway, Burnaby, British Columbia, Canada V5H2E4.